Effect of Compressive Stresses on Leakage Currents in Microchip Tantalum Capacitors

Alexander Teverovsky

Dell Services Federal Government, Inc
NASA/GSFC, Code 562, Greenbelt, MD 20771
Alexander.A.Teverovsky@nasa.gov

Abstract

Microchip tantalum capacitors are manufactured using new technologies that allow for production of small size capacitors (down to EIA case size 0402) with volumetric efficiency much greater than for regular chip capacitors. Due to a small size of the parts and leadless design they might be more sensitive to mechanical stresses that develop after soldering onto printed wiring boards (PWB) compared to standard chip capacitors. In this work, the effect of compressive stresses on leakage currents in capacitors has been investigated in the range of stresses up to 200 MPa. Significant, up to three orders of magnitude, variations of currents were observed after the stress exceeds a certain critical level that varied from 10 MPa to 180 MPa for capacitors used in this study. A stress-induced generation of electron traps in tantalum pentoxide dielectric is suggested to explain reversible variations of leakage currents in tantalum capacitors. Thermo-mechanical characteristics of microchip capacitors have been studied to estimate the level of stresses caused by assembly onto PWB and assess the risk of stress-related degradation and failures.
Keywords: tantalum capacitors, leakage current, soldering, reliability, mechanical stress.

Introduction

One of the major trends in the electronic industry is further micro-miniaturization of devices, assemblies, and parts that requires production of high performance, efficient, and economical components within a smaller volume. To answer the request for downsizing, manufacturers of tantalum capacitors recently developed new technologies to produce small size capacitors with increased volumetric efficiency that might replace with time conventional design tantalum capacitors that have been manufactured for more than 30 years. Microchip tantalum capacitors were originally developed for commercial mobile wireless devices such as handheld computers, smartphones, cameras, etc., but provided the parts have adequate quality and reliability, their application would be beneficial for space systems allowing for reduction of weight and size of assemblies and units.

Currently, small size tantalum capacitors (EIA size code 0603 and 0402) are commercially available from Vishay and AVX and expanding successfully to areas of application where ceramic capacitors were traditionally used.

Although conventional chip tantalum capacitors are considered high volumetric efficiency devices, only ~ 30% of their volume is occupied by tantalum [1] and the rest is “wasted” mostly for the lead frame and molding compound (MC). New technologies increase volumetric efficiency further, up to ~ 45% for TM8 (Vishay) series and up to 54% for TAC (AVX) series devices [2]. Figure 1 shows cross-sectional views of a regular chip tantalum capacitor with anode slug sintered around a tantalum wire, and two designs of microchip capacitors, one with a welded anode riser wire (Mfr.B) and another with the tantalum slug sintered directly to the tantalum wafer used as anode terminal (Mfr.A). A substantial improvement in the volumetric efficiency is achieved by a new design of

anode and cathode interconnections with terminals that eliminates internal welding between the lead and anode wire.

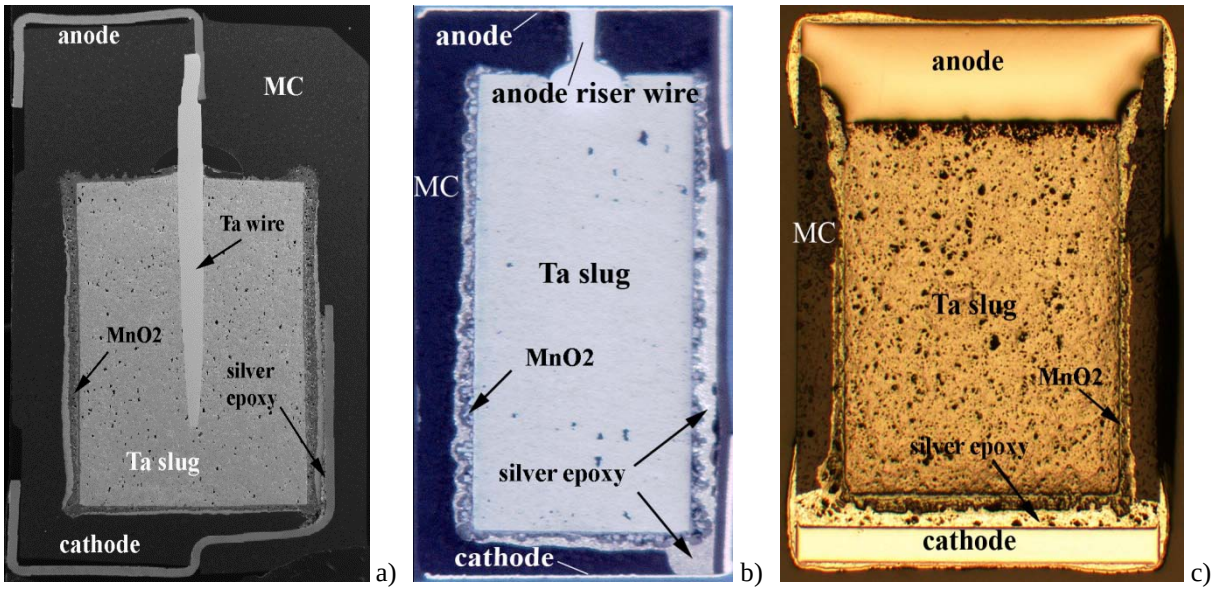

Figure 1. Cross-sectional views of a regular tantalum chip capacitor (a) and microchip capacitors (b, c). Note that the pictures are not in the same scale.

Our previous study [3] showed for that compressive stresses might substantially degrade characteristics of tantalum capacitors and cause failures. Leakage currents in regular chip capacitors under compressive stress increased more than two orders of magnitude and surge current breakdown voltages were up to 40% less than for unstressed parts. Different part types had different sensitivity to mechanical stresses, and average levels of critical stresses varied from 10 MPa to 40 MPa. The most intriguing feature of the stress-induced degradation was the reversibility of current variations and hysteresis during measurements at increasing and decreasing forces. However, the details and the origin of this reversibility have not been fully determined. It was not clear whether the effect is related to specifics of the design of capacitors, to local stresses in the slug around the tantalum wire, or to stresses that are transferred through the molding compound and distributed more-or-less evenly in the slug. Microchip capacitors that eliminate relatively loose connections between anode wires and slugs either by welding or by replacing the wire with a tantalum plate provide more convenient structures for testing and analysis.

Microchip capacitors do not have leads that might provide some stress relief, and their cross-sectional area and thickness of the encapsulating molding compound are smaller compared to regular chip tantalum capacitors. This makes them potentially more susceptible to the effect of mechanical stresses. In this work, variations of leakage currents in different types of microchip tantalum capacitors with compressive stresses were studied to assess the level of critical stresses and get insight into the mechanism of the phenomenon. Thermo-mechanical (coefficients of thermal expansion, CTE) and mechanical (Young's modulus) characteristics of the parts were measured to estimate soldering-induced mechanical stresses in microchips and evaluate the risk of degradation caused by assembly onto PWBs.

Experiment

Seven types of microchip tantalum capacitors from two manufacturers were used in this study. The parts had different design and size and were selected to verify and assess the effect of compressive stresses in capacitors where the strain can be transferred directly to the slug either via a welded tantalum wire (Mfr.B) or

through a thin layer of manganese oxide and silver epoxy (Mfr.A).

Table 1. Microchip tantalum capacitors

Group	Mfr	C, uF	VR, V	case	DCL, μA	L, mm	W, mm	H, mm
1	A	33	10	A (1206)	3.3	3.2	1.6	1.6
2	A	33	10	R (0805)	3.3	2.1	1.4	1.4
3	A	1	35	R (0805)	0.5	2.1	1.4	1.4
4	A	10	10	R (0805)	1	2.1	1.4	1.4
5	B	10	16	A(1206)	0.8	3.4	1.7	1.7
6	B	47	10	T	2.35	3.5	2.8	1.5
7	B	4.7	6.3	M	0.16	1.6	0.85	0.85

Table 1 shows description of the parts including their specified electrical characteristics capacitance, C, rated voltage, VR, DC leakage, DCL, and size (length, L, width, W, and thickness, H).

In this study, leakage currents of capacitors were monitored under the stresses changing with time. A stress created by a compressed spring was applied to the terminals of the parts and its level was monitored by a force gauge. A PC-based data acquisition system that is shown in Figure 1 allowed for programming of stress and voltage variations with time and for recording the values of applied force and leakage currents.

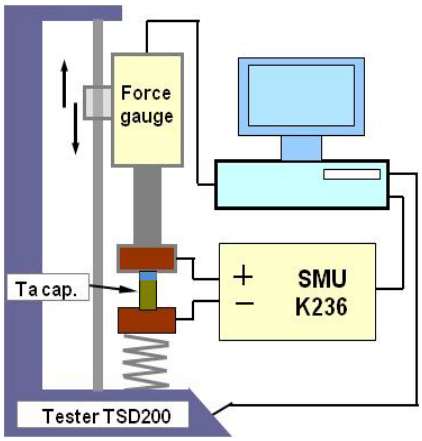

Figure 1. Experimental set-up for programming stress and voltage profiles and monitoring leakage currents in microchip capacitors with time.

Coefficients of thermal expansion of microchip tantalum capacitors were calculated based on measurements of deformation of the parts with temperature using a thermo-mechanical analyzer, TMA2940, manufactured by TA Instruments. The deformation was measured along the terminals at a rate of 3 °C/min. during cooling from 220 °C to room temperature.

To assess the effective Young's modulus, *E*, of the capacitors and tantalum anodes (slug) deformation of the parts and the level of applied load were recorded using an Instron Model 4442 tester. Measurements were carried out at compressive forces up to 250 N during increasing and decreasing load at a speed of 0.005 inch/minute.

Results

Effect of mechanical stresses on leakage currents.

Typical experimental results for different part types showing variations of leakage currents with time at rated voltages and varying compressive stresses are shown in Figures 2 to 4. Electro-mechanical behavior of microchip capacitors is similar to what was observed for regular tantalum capacitors and indicates that compression might substantially, in some cases up to three orders of magnitude (see Figure 4a), increase leakage currents. After the stress removal, the currents might recover completely (see Figures 2a, 3b, and 4b) or partially, decreasing noticeably, but not to the initial level (see Figures 2b, 3a). The results show that the effect is not specific to the design of the parts and is likely an intrinsic characteristic of the anodically grown tantalum pentoxide dielectric.

In some cases, currents increased instantaneously from ~ 10^{-9} A to ~10^{-5} A, as in Figure 2b, sharply drop to ~10^{-7} A and then gradually decrease back to the

nanoampere level. The sharp spike is likely due to a scintillation breakdown caused by mechanical damage to the tantalum pentoxide dielectric. However, in most cases currents increased gradually, remained relatively stable when the stress was stabilized, and then decreased as the force lowered to the "safe" level of 5 N that was used to maintain electrical contacts to the part. A delay in stabilization of currents is clearly seen in Figures 3b and 4b where the current levels off in approximately 1.5 min after stabilization of the stress.

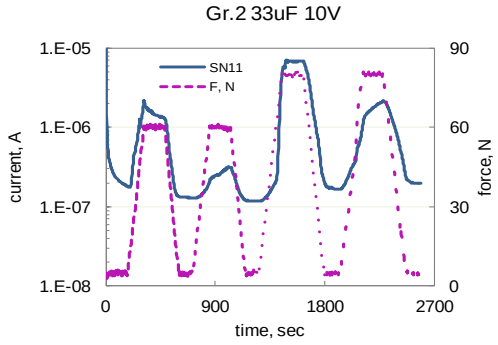

a)

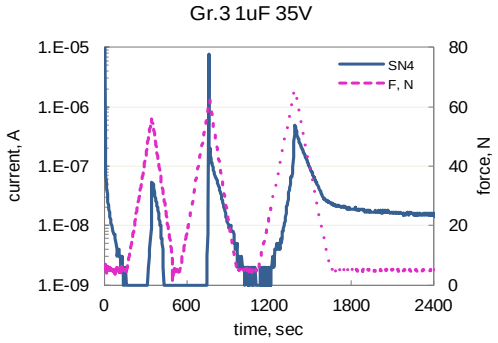

b)

Figure 2. Effect of compressive stresses on Gr.2 and Gr.3 microchip capacitors. Here and below leakage currents were measured at rated voltages.

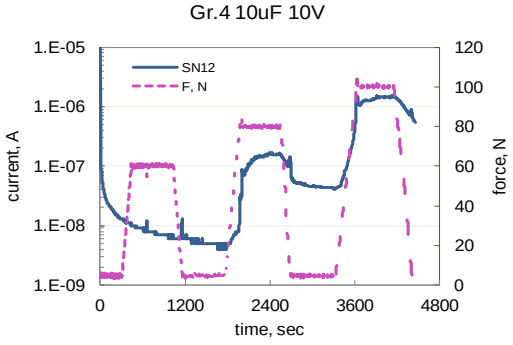

a)

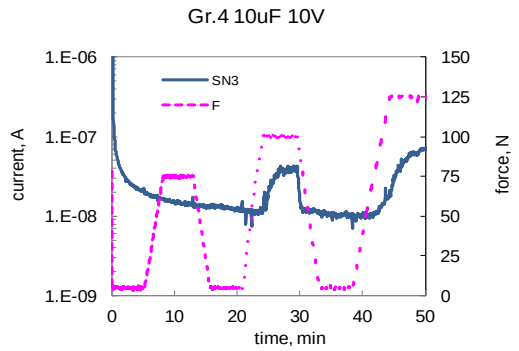

b)

Figure 3. Variations of leakage currents with compressive stresses in Gr.4 microchip capacitors.

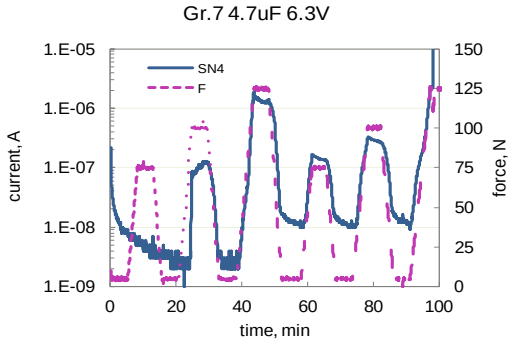

a)

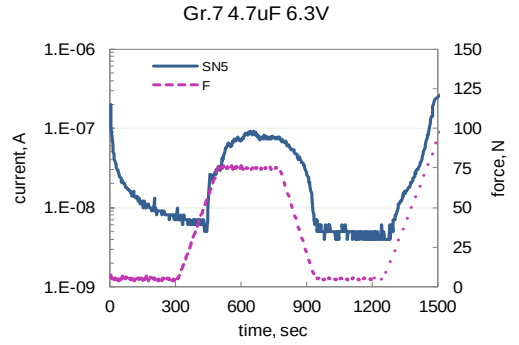

b)

Figure 4. Variation of leakage currents with compressive stresses Gr.7 microchip capacitors.

To evaluate I-V characteristics in compressed capacitors, currents were monitored after application of different voltages for 3 to 5 minutes untill stabilization. Typical I-V characteristics of microchip capacitors in initial and stressed conditions are shown in Figure 5. Experimental data can be approximated with straight lines in coordinates *ln(I/V) vs.* $V^{0.5}$ indicating bulk-limited Poole-Frenkel (PF) conduction that is due to electrons released to a conduction band from traps in the forbidden energy gap of the oxide.

According to the PF model current density through a dielectric can be presented as follows:

$$J = C_t E \exp\left(-\frac{qU}{kT}\right)\exp\left(\frac{\tilde{\beta}_{PF} E^{1/2}}{kT}\right) \quad (1)$$

where C_t is a trap density related constant, E is the electric field, q is the charge of electron, U is the barrier height, k is the Boltzmann constant, T is the absolute temperature; and

$$\tilde{\beta}_{PF} = \frac{\beta_{PF}}{r} = \frac{1}{r}\left(\frac{q^3}{\pi\varepsilon_0\varepsilon}\right)^{1/2}$$

is the effective PF constant, ε_0 is the permittivity of the free space, and ε is the high-frequency dielectric constant, which for Ta2O5 is ≈ 5. Constant r is the compensation coefficient that can vary from 1 to 2 and accounts for multi-level traps and partial compensation of donor centers [4-5]. Calculations based on the slopes of lines in Figure 5 yield $1.3 \le r \le 1.6$, which is close to the theoretical values, and confirm PF conduction for both, compressed and unstressed capacitors.

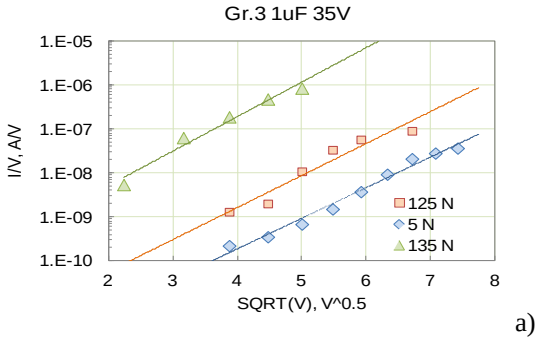

a)

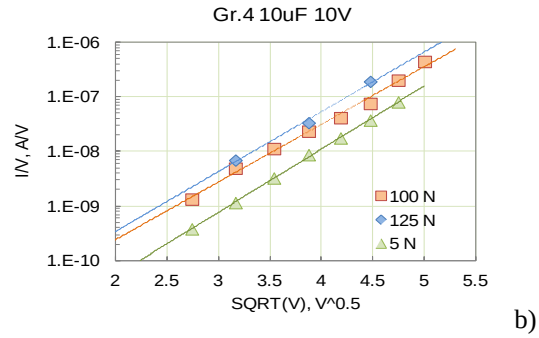

b)

Figure 5. Effect of stress on I-V characteristics of Gr.3 (a) and Gr.4 (b) capacitors. Legends indicate the level of compressive stresses during the measurements.

Based on test results similar to those shown in Figures 2 to 4, the values of critical forces, F_{cr}, that were determined as force corresponding to a two-fold increase in leakage currents were determined for each capacitor. The relevant critical stresses, σ_{cr}, were calculated as a ratio of F_{cr} to the cross-sectional area of the part. Distributions of critical stresses are shown in Weibull coordinates in Figure 6. In most cases the distributions could be approximated by two-parameter Weibull functions with slopes, β, varying in a relatively narrow range, from 3 to 4. Similar slopes for different part types indicate that likely the same mechanism is responsible for the stress-induced degradation of leakage currents in all part types. The characteristic critical stress, η, for different groups of capacitors varied in a wide range from 33 MPa to 156 MPa.

One sample in group 2 was "out of family" showing DCL degradation at a stress of 10 MPa that was more than 3 times less than for the other samples in this group.

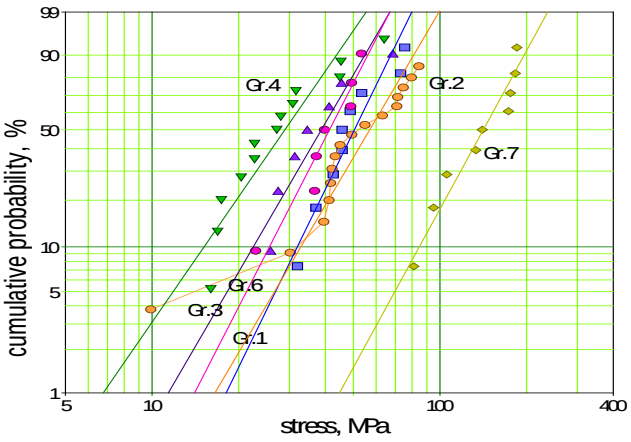

Figure 6. Distributions of critical stresses in different types of microchip tantalum capacitors. Note that one sample in group 2 had a substantially lower level of the critical stress compared to the rest of the samples.

Table 2 displays parameters of distributions of the critical stresses. Average values of σ_{cr} for all groups, except for Gr.7, were in a range, from 30 MPa to 60 MPa that is slightly greater than what was observed for regular chip tantalum capacitors [3]. Interestingly, the smallest size capacitors, Gr.7, had the largest values of σ_{cr} that vary from 81 MPa to 185 MPa.

Table 2. Characteristics of distributions of the critical stresses (MPa) in microchip tantalum capacitors.

Lot	QTY	β	η	Mean	STD	max	min
Gr.1	9	4.1	55.2	50.1	13.7	75.4	32.0
Gr.2	18	2.2	66.5	58.9	28.0	87.0	9.9
Gr.3	7	3.5	43.1	38.7	12.4	68.6	25.8
Gr.4	13	2.9	32.8	29.3	10.9	64.0	16.0
Gr.6	7	3.9	45.4	41.1	11.7	53.4	22.9
Gr.7	9	3.7	156.3	141.0	42.7	185.0	81.1

Thermo-mechanical characteristics.

Typical results of measurements of deformations for four types of capacitors are shown in Figure 7. The expansion of tantalum microchip capacitors with temperature might be approximated with straight lines and in this respect is similar to deformation of molding compounds (MC) that exhibit two distinctive areas of deformation: low-temperature glassy state and high-temperature rubbery state. The interception point of these lines indicates the effective glass transition temperature (Tg_eff) of the molding compound and the slopes of the lines indicate the effective values of coefficients of thermal expansion (CTE) of capacitors. Both parameters depend on the relative size, Young's modulus, and CTE values of the MC and tantalum slug.

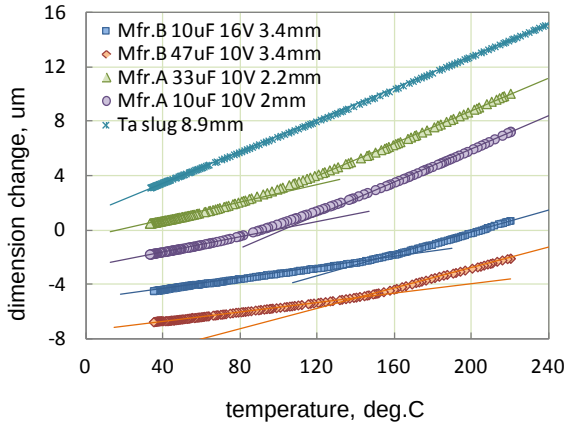

Figure 7. Thermo-mechanical characteristics of four types of microchip capacitors and a tantalum slug. The legend indicates the length of the samples used.

To evaluate the contribution of the slug and MC to the deformation of capacitors, thermo-mechanical characteristics of a tantalum slug, a regular chip capacitor (15uF 50V, case size D), and a piece of MC cut from the case were measured. Results of these measurements as well as CTE values at low temperatures, T < Tg_eff, CTE1, and at high temperatures, T > Tg_eff, CTE2, are summarized in Table 3. Considering the accuracy of Tg measurements of ±5 °C the data for a regular chip capacitor and its MC are close. The value of CTE for a tantalum slug, ~ 6.1 ppm/°C, is close to the literature data for tantalum (6.3 ppm/ ^{o}C) thus indicating that the presence of Ta2O5 dielectric does not affect substantially temperature deformations of the slug. At a CTE of the slug much smaller than of the molding compound, deformation of MC in capacitors is constrained and the measured CTE are reduced on 30% to 45% compared to the MC. This reduction might be even more substantial for microchip capacitors because of the smaller volume of MC used.

The parts manufactured by the same vendor had similar characteristics indicating that the same molding compound was used for different part types. The molding compound used by Mfr. A had a relatively low glass transition temperature ~105 ^{o}C and relatively large values of the effective CTE: 13.5 ±1.3 ppm/^{o}C at low temperatures and ~32 ±4.3 ppm/^{o}C at high temperatures. Mfr. B employed high-Tg molding compound (~150 ^{o}C) and capacitors had lower CTE values that were close to CTE of tantalum slug at T < 150 ^{o}C, 6.5 ±1 ppm/^{o}C. At temperatures exceeding Tg the values of CTE still remain low, ~16.5 ±5 ppm/^{o}C.

Direct experiments performed in [6] showed that the CTE mismatch between materials used in the construction of a tantalum capacitor can cause leakage current failures after soldering. When soldering simulation was carried out with unencapsulated devices no changes in leakage currents were observed;

however, failures occurred when this experiment was repeated after plastic encapsulation. A difference between the CTE for microchips and tantalum slug for Mfr.A indicates that substantial mechanical stresses in the slug might develop under temperature excursions (e.g. temperature cycling or soldering-related thermal shock), cause damage to Ta2O5 dielectric and failures.

Table 3. Thermo-mechanical characteristics of tantalum capacitors.

Capacitor/ Material	Mfr.	CTE1, ppm/°C	CTE2, ppm/°C	Tg_eff, °C	E, GPa**
Gr.1	A	11.2	31	110	10
Gr.2	A	13.9	28.8	100.2	5
Gr.3	A	13.6	38	101.4	
Gr.4	A	14.1	28.9	108.4	
Gr.5	B	5.7	12	147.9	15
Gr.6	B	5.85	10.9	156.5	10
Gr.7	B	6.6	19.8	153.9	10
Ta slug*	-	5.7	6.5	-	15
15uF 50V cap	C	14	56	165	-
15uF 50V MC	-	20	75	155	-

*CTE1 for Ta slug corresponds to the range of temperatures from 22 °C to 150 °C, and CTE2 to the range from 150 °C to 300 °C.

** conservative estimations.

Unfortunately, an attempt to measure the effective Young's modulus, *E*, of the capacitors was not successful because the stiffness of the parts was relatively large and the measured deformations were close to the deformation of the frame with the gage. This allowed for a rough estimation of the minimal level of *E* only. Results of these estimations are presented in Table 3 and indicate *E* in the range from 5 GPa to 15 GPa. This range is consistent with the literature data for Young's modulus of epoxy molding compounds (from 1 GPa to 20 GPa) and for porous tantalum materials (from 15 GPa to 20 GPa) with the pore volume fraction between 27% and 55% [7]. Note that the Young's modulus of solid tantalum at room temperature is much greater, ~ 190 GPa.

Discussion

Leakage currents in tantalum capacitors.

Excessive leakage currents in tantalum capacitors are often attributed to the presence of defects in the dielectric created by rupture of the tantalum pentoxide layer under high mechanical stresses [8]. Fagerholt [9] suggested that stresses applied to the part can drive sharp manganese dioxide (MnO2) crystals in the cathode layer (see Figure 8) to penetrate and impair the dielectric resulting in scintillations or increasing leakage currents in the capacitors.

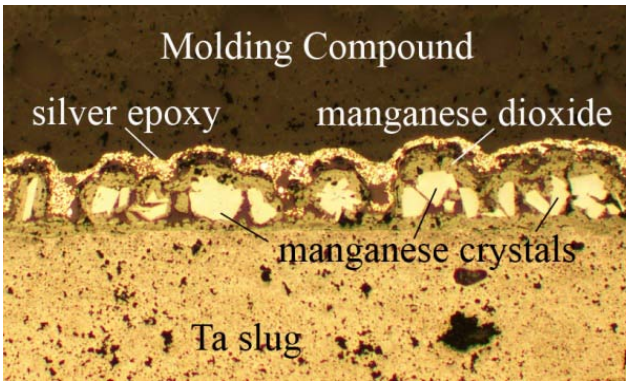

Figure 8. Cross-section of a tantalum capacitor showing crystals in the manganese oxide cathode layer.

Scintillations, or local breakdowns terminated by conversion of the conductive MnO2 into a high-resistive Mn2O3 phase due to local heat dissipation,

result typically in high current spikes that were also observed during our experiments. However, this mechanism cannot explain stabilization of leakage currents at a constant level of stress and their recovery after the stress is released.

Additional experiments (see Figure 9) showed that the effect of stress is not specific to the parts with manganese cathodes, but can be also observed in capacitors with cathodes made of conductive polymers. In addition, the independence of the effect from specifics of the design of tantalum capacitors, indicates that the stress-induced degradation of leakage currents is an intrinsic feature of the sintered tantalum/tantalum pentoxide system. A possible explanation for this phenomenon is a stress-induced generation of electron traps that increases conductivity of the tantalum pentoxide dielectric in areas where high local compressive stresses are developed.

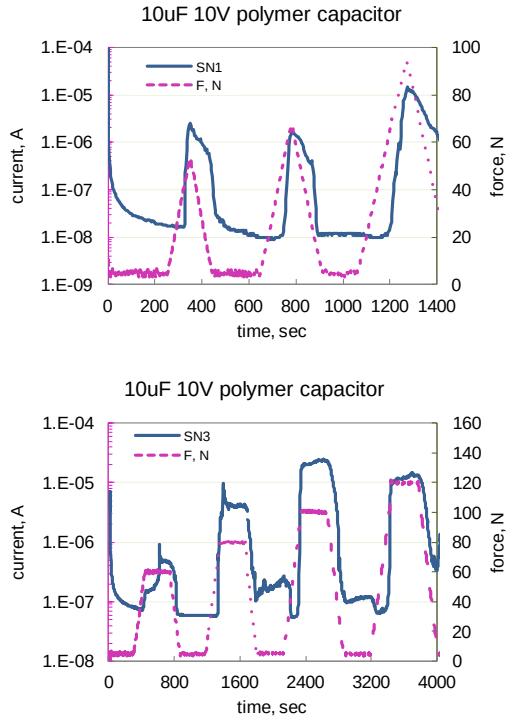

Figure 9. Variations of leakage currents in polymer 10 μF 10 V tantalum capacitors (case size A, 3216-18) under compressive stresses. The level of critical stress for these parts is 15 MPa and 20 MPa.

Multiple studies have shown that the electron transport in tantalum pentoxide dielectrics is due either to a bulk-limited Poole-Frenkel conduction or to surface-barrier-limited Schottky mechanisms [4, 10-12]. It is assumed that different conduction mechanisms can prevail at different ranges of voltage and temperature, and can vary depending on the treatment of the oxide (e.g. annealing conditions) [13-14]. Simmons proposed a modified Schottky mechanism according to which the current depends on the surface barrier level and the mobility of electrons in the bulk of dielectric [15]. The surface-barrier-limiting mechanism is likely prevailing at relatively low electric fields, while the bulk-limiting mechanism is prevailing at high voltages and currents [13, 16-17]. A detailed analysis of different conduction mechanisms in Ta2O5 dielectrics was performed by Novkovski and Atanassova [18]. Anodic tantalum oxide films have a disordered structure and a substantial amount of electron traps, up to 10^{19} cm^{-3}, so electron transport through the oxide at sufficiently large electric fields is commonly described as Poole-Frenkel conduction.

Our experimental data can be explained assuming that the electron transport is bulk-limited and increases with the concentration of electron traps as predicted per Eq.(1). Mechanical stresses result in formation of microscopic defects such as broken Ta-O bonds or generation of oxygen vacancies. This increases the concentration of traps in the dielectric, might result in formation of the trap-related conductive band and raise leakage currents in the capacitors. A similar mechanism related to the Si-O bonds breaking due to physical stresses in silicon dioxide was used to explain factors affecting leakage currents and reliability of gate oxides in microcircuits [19-20].

The reversibility of the process of current degradation in capacitors can be explained assuming that the trap concentration is determined by a dynamic equilibrium of two competitive processes: generation of stress-induced defects and their annealing (e.g., recombination of the broken bonds). When the stress is removed, the concentration of the traps returns to its initial value and so does leakage current. Both processes, generation under the stress and recombination after stress removal develop with time resulting in delays and hysteresis during stress cycling that was observed in our experiments.

Due to a irregular, sponge-like structure of the tantalum anode, the level of stress that causes trap generation in Ta2O5 dielectrics is likely much greater than the measured critical stress in the part. Repeat applications

of compressive stresses after recovery of currents in some cases increased currents to a lesser degree. Assuming that the increased DCL is due to local areas with sufficiently high level of stress, a reduction of the sensitivity to stress might be due to some non-reversible deformations in the part that does not allow restoring the same level of local stresses as developed initially. However, for some capacitors the sensitivity increased during the following cycles. This behavior is also consistent with the model assuming that the level of local stresses is the same, but the trap concentration was not annealed completely during the relaxation period, so the starting level for traps' generation is greater for the following cycle.

A trend of increasing of σ_{cr} for parts with smaller case size might be explained assuming that the stress-induced degradation of leakage currents is associated with the presence of some macro-structural defects in the parts, e.g. bumps or burrs on the surface of the tantalum slug. These macro-defects have a high sensitivity to mechanical stresses, but are relatively small and their size does not depend on the dimensions of the part. In this case, capacitors with different size but similar macro-defects would have close critical forces; however, the critical stress would be less for large size capacitors.

Estimations of stresses caused by soldering onto PWBs

During soldering of a capacitor onto a printed wiring board both, the part and the board, are heated up to temperatures above the melting point of solder (typically to ~ 230 ^{o}C for eutectic Sn/Pb solder) which solidifies when the system is cooled down to room temperature. Due to differences of the coefficients of thermal expansion between the part and PWB, mechanical stresses are building up as the temperature decreases below the point of solidification of solder. However, when the temperature remains above the glass transition temperature of the PWB, Tg, the level of stresses is relatively low and for rough estimations we can assume that the stresses are formed only after temperature decreases below Tg.

To estimate these stresses let us consider a schematic of a microchip tantalum capacitor soldered onto a PWB shown in Figure 10. For a simplified one-dimensional model, assuming that materials follow Hooke's law, and that the temperature variations of Young's modulus, E, and CTE, α_{PWB}, in the glassy state can be neglected, the compressive stress that develops in a soldered capacitor after cooling to room temperature, T_r, can be expressed as:

$$\sigma = \frac{(\alpha_{PWB} - \alpha_{cap}) \times (T_g - T_r)}{(E_{cap})^{-1} + \left(E_{PWB} \times A_{PWB} / A_{cap}\right)^{-1}} \quad , \qquad (2)$$

where A_{cap} and A_{PWB} are the cross-sectional areas of the capacitor and PWB, α_{cap} is the low-temperature coefficient of thermal expansion of the capacitor, and E_{cap} and E_{PWB} are the values of their effective Young's modulus.

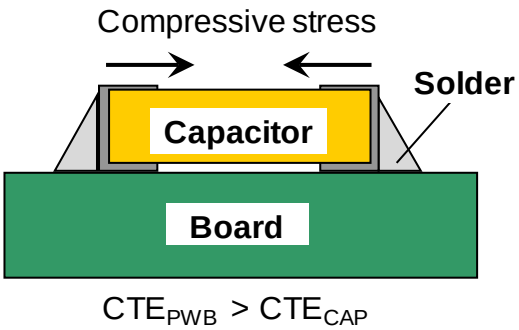

Figure 10. Stresses developed in a microchip tantalum capacitor after soldering.

Based on the literature data [21] and results of our measurements, parameters of epoxy-based (FR4) and polyimide-based (PI) boards and microchip tantalum capacitors are summarized in Table 4. The areas of the capacitor and board were calculated as a product of their thicknesses and widths, $A_{cap} = h_{cap} \times W_{cap}$ and $A_{PWB} = h_{PWB} \times W_{cap}$. Results of calculations per Eq.(2) for different part types and a board of a thickness of 1/8 inch (3.175 mm) are presented in Table 5.

Table 4. Mechanical characteristics used for stress calculations.

Characteristic	FR4	PI	microchip
Tg, ^{o}C	145	230	
CTE, ppm/^{o}C	15	12.4	Per Table 3
E, Gpa	17.5	23.5	10

The stresses for Mfr.B capacitors soldered onto a polyimide board are slightly greater compared to FR4 board, which is due to a higher Tg value for PI.

Tensile stresses for Mfr.A capacitors (Gr.2 to Gr.4) assembled onto PI board are due to relatively large CTE of these parts that exceed CTE of polyimide and can cause fractures in the attachment and open circuit failures. The smallest size capacitors from Gr.7 have the greatest margin between the minimal observed critical stress (81.1 MPa) and the level of stresses that might be caused by soldering onto a PI board (~11 MPa). Calculations using Eq.(2) show that even a twofold increase of the thickness of the board (to ¼ inch) only slightly, from 6% to 13%, raises the level of stresses in the capacitors, so soldering-induced stresses will not cause degradation of leakage currents and failures for normal quality microchip tantalum capacitors.

Table 5. Calculated mechanical stresses in microchip capacitors.

Gr.	W, mm	H, mm	CTE, ppm/^{o}C	A_{cap}, m^2	A_{PWB}, m^2	σ_FR4, Mpa	σ_PI, Mpa
1	1.6	1.6	11.2	2.6E-6	4.8E-6	3.6	2.0
2	1.4	1.4	13.9	1.9E-6	4.2E-6	1.1	-2.6
3	1.4	1.4	13.6	1.9E-6	4.2E-6	1.4	-2.1
4	1.4	1.4	14.1	1.9E-6	4.2E-6	0.9	-2.9
5	1.4	1.4	5.7	1.9E-6	4.2E-6	9.2	11.5
6	2.8	1.5	5.85	4.2E-6	8.4E-6	8.9	11.1
7	0.85	0.85	6.6	7.2E-7	2.5E-6	9.0	10.6

Results show that the level of soldering-induced compressive stresses can exceed 10 MPa, and although a sufficient margin exists between the critical level of stresses and stresses developed after soldering, for some parts with defects the level of critical stresses might be low enough to degrade their characteristics and cause failures after soldering. A special care should be taken to assure the necessary margin in lots of microchip capacitors used for high-reliability applications. A qualification testing that includes measurements of leakage currents under a stress of 10 MPa might be used for this purpose.

Conclusion

1. Compressive stresses can result in increase of leakage currents in microchip tantalum capacitors up to three orders of magnitude. The characteristic value of critical stresses in different part types varies from 35 MPa to 160 MPa and the slopes of Weibull distributions are in the range from 2.2 to 4.1. However, some defective capacitors might degrade at relatively low stresses, ~10MPa, that are substantially below the average level.
2. Similar to regular chip tantalum capacitors, stress-induced degradation in microchip capacitors is reversible: leakage currents increase gradually with stress, remained relatively stable when the stress is stabilized, and then decrease as the stress is lowered. This behavior is explained assuming a bulk-limited Poole-Frenkel mechanism of conduction and stress-induced generation of electron traps that increases conductivity of the tantalum pentoxide dielectric.
3. Thermo-mechanical characteristics (effective Tg and CTE) for parts from different vendors vary substantially from ~105 ^{o}C to ~ 150 ^{o}C (Tg) and from ~6.5 ppm/^{o}C to ~13.5 ppm/^{o}C (CTE at T < Tg). Considering that CTE for a tantalum slug is ~6.2 ppm/^{o}C, different part types might experience different level of thermo-mechanical stresses during temperature excursions and have different reliability under temperature cycling conditions.
4. Analysis of mechanical stresses in microchips after soldering caused by the CTE mismatch between boards and capacitors showed that for both, polyimide and FR4 boards, the level of estimated

stresses is relatively low, and for normal quality parts a sufficient margin exists between the critical level of stress and stresses developed after soldering.

Acknowledgments

This work was sponsored by NASA Electronic Parts and Packaging (NEPP) program. The author is thankful to Michael Sampson (GSFC), NEPP Program Manager, for support of this investigation, to Justin Jones (GSFC) for help with Young's modulus measurements, and to manufacturers of tantalum capacitors for presenting samples for this study.

References

[1] A. Eidelman and P. Vaisman, "Addressing Tantalum Capacitors Technology Challenges," presented at the CARTS USA, Albuquerque, NM, 2007, March 26-29.

[2] W. Millman and D. Huntington, "Tantalum Capacitors Bring Micro-Miniaturisation to Electronic Devices," presented at the CARTS USA, Albuquerque, NM, 2007, March 26-29.

[3] A. Teverovsky, "Effect of mechanical stresses on characteristics of chip tantalum capacitors," *IEEE Transactions on device and materials reliability*, vol. 7, pp. 399-407, 2007.

[4] E. Atanassova and A. Paskaleva, "Conduction mechanisms and reliability of thermal Ta2O5–Si structures and the effect of the gate electrode," *Journal of Applied Physics*, vol. 97, pp. 1-11, 2005.

[5] D. Spassov, E. Atanassova, and D. Virovska, "Electrical characteristics of Ta2O5 based capacitors with different gate electrodes," *Applied Physics a-Materials Science & Processing*, vol. 82, pp. 55-62, Jan 2006.

[6] R. Hahn, J. Piller, and P. Lessner, "Improved SMT Performance of Tantalum Conductive Polymer Capacitors with Very Low ESR," in *The 26th symposium for passive components, CARTS'06*, Orlando, FL, 2006, pp. 291-303,

[7] V. K. Balla, S. Bodhak, S. Bose, and A. Bandyopadhyay, "Porous tantalum structures for bone implants: Fabrication, mechanical and in vitro biological properties," *Acta Biomaterialia*, vol. 6, pp. 3349-3359, Aug 2010.

[8] R. W. Franklin, "An exploration of leakage current," in *Electronic Components and Technology Conference, 1990. Proceedings., 40th*, 1990, pp. 1002 - 1007,

[9] P. Fagerholt, "A new view on failure phenomena in solid tantalum capacitors," in *16th Capacitors and Resistors Technology Symposium, CARTS'96*, 1996, pp. 162-166,

[10] F. Chiu, J. Wang, J. Lee, and S. Wu, "Leakage currents in amorphous Ta2O5 thin films," *Journal of Applied Physics*, vol. 81, pp. 6911-6915, 15 May 1997 1997.

[11] R. Ramprasad, "Phenomenological theory to model leakage currents in metal-insulator-metal capacitor systems," *Physica Status Solidi B-Basic Research*, vol. 239, pp. 59-70, Sep 2003.

[12] E. Loh, "DC conduction mechanism in tantalum chip capacitors," *Journal of Physics D-Applied Physics*, vol. 13, pp. 1101-1111, 1980.

[13] S. Ezhilvalavan and T. Tseng, "Conduction mechanisms in amorphous and crystalline Ta2O5 thin films," *Journal of applied physics*, vol. 83, pp. 4797-4801, 1998.

[14] E. Atanassova and A. Paskaleva, "Breakdown fields and conduction mechanisms in thin Ta2O5 layers on Si for high density DRAMs," *Microelectronics Reliability*, vol. 42, pp. 157-173, 2002.

[15] J. G. Simmons, "Richardson-Schottky effect in solids," *Physical Review Letters*, vol. 15, pp. 967-968, 1965.

[16] J. G. Simmons, "Transition from Electrode-Limited to Bulk-Limited Conduction Processes in Metal-Insulator-Metal Systems," *Physical Review*, vol. 166, pp. 912-920, 1968.

[17] M. J. Lee and K. S. Chung, "Effects of Postannealing on Current-Voltage Characteristics of Metal-Insulator(Ta2O5)-Metal Type Thin-Film Diodes," *Journal of the Korean Physical Society*, vol. 39, pp. 686-691, 2001.

[18] N. Novkovski and E. Atanassova, "A comprehensive model for the I-V characteristics of metal-Ta2O5/SiO2-Si structures," *Applied Physics a-Materials Science & Processing*, vol. 83, pp. 435-445, Jun 2006.

[19] T. C. Yang and K. C. Saraswat, "Effect of physical stress on the degradation of thin SiO(2) films under electrical stress," *Ieee Transactions on Electron Devices*, vol. 47, pp. 746-755, Apr 2000.

[20] Y. Nakajima, T. Toda, T. Hanajiri, T. Toyabe, and T. Sugano, "In-depth profiling of electron trap states in silicon-on-insulator layers and local mechanical stress near the silicon-on-insulator/buried oxide interface in separation-by-implanted-oxygen wafers," *Journal of Applied Physics*, vol. 108, pp. 124505-124505-5, 2010.

[21] H. Y. Qi, S. Ganesan, J. Wu, M. Pecht, P. Matkowski, and J. Felba, *Effects of printed circuit board materials on lead-free interconnect durability*. New York: Ieee, 2005.